Perspectives of strangeness measurements at LHC with ALICE

Antonin Maire for the ALICE Collaboration,

Institut pluridisciplinaire Hubert Curien (IPHC), 23 rue du loess - 67037 Strasbourg, France

DOI: http://dx.doi.org/10.3204/DESY-PROC-2010-01/212

In November 2009, the Large Hadron Collider produced its first proton-proton collisions at the centre of mass energy ($\sqrt{s}$) of 900 GeV. Since then, several hundred million of 7 TeV collisions have been recorded by the ALICE experiment. The low material budget of the ALICE sub-detectors in the central rapidity region and the excellent particle identification capabilities allow the extraction of transverse momentum (p_{T}) spectra for a range of identified particles. In this presentation, we report p_{T} measurements (uncorrected spectra) for strange and multi-strange particles (i.e. ϕ, $\mathrm{K}^0_{\mathrm{S}}$, Λ^0, $\overline{\Lambda}^0$, Ξ and Ω), identified via topological methods.

1 Introduction and motivation

Strange particle production in proton-proton (pp) collisions is a necessary benchmark for the physics of ultra relativistic heavy ions. This is important at the Large Hadron Collider (LHC), where the heavy-ion programme is scheduled to begin in the late 2010 [1]. Moreover, strangeness in pp collisions is interesting in itself, as it may shed light on hadron production mechanisms. While the *hard* component of the event may be described by the perturbative Quantum Chromo-Dynamics (based on parton-parton scattering and fragmentation [2, 3]), the *soft* component must be treated in a more complex manner. Currently, the soft physics is described via thermal models [4, 5] or via QCD-inspired models (relying on multi-parton processes [6] or multiple scattering [7, 8], for instance). In either case, further improvements of such phenomenological models may be spurred by confrontation with experimental measurements.

In that respect, strange and multi-strange particles (ϕ, $\mathrm{K}^0_{\mathrm{S}}$, Λ^0, $\overline{\Lambda}^0$, Ξ, Ω, ...), which are the focus of this publication, may provide the relevant insights: due to identification via decay topology reconstruction, they can be studied over a large momentum range. Starting from $p_{\mathrm{T}} \approx 0.2$ GeV/c and up to ≈ 10 GeV/c, these spectra cover the region dominated by the soft processes and reach the energy scale where hard scattering mechanisms dominate.

Some measurements have already been performed at previous and current facilities. These include both the $\mathrm{p\overline{p}}$ colliders (Sp$\overline{\mathrm{p}}$S, Tevatron) and a pp collider (RHIC), with centre of mass energies $\sqrt{s}$ ranging from 200 GeV up to 1.96 TeV [9–18]. The LHC having been in operation since November 2009, it is now possible to extend the existent 900-GeVmeasurements made by the UA1 and UA5 collaborations in $\mathrm{p\overline{p}}$, and to perform new measurements at $\sqrt{s} = 7$ TeV, beyond the Tevatron energies.

The ALICE experiment [1] is well-suited for such spectrum measurements, due to a low

p_{T} cut-off and excellent particle identification (PID) capabilities. The low p_{T} cut-off is made possible by the low magnetic field applied in the central barrel ($\leq 0.5\ T$) and the low material budget in this mid-rapidity region (13% of radiation length [19]). The PID capabilities are supplied by a set of detectors utilizing diverse techniques (energy loss, transition radiation, Cerenkov effect, time of flight).

2 Data analysis and identification methods

2.1 Data collection and detector setup

The data presented here is from the minimum bias sample collected during the Nov-Dec 2009 LHC pp run at $\sqrt{s} = 900$ GeV [20] ($\sim 3 \times 10^5$ events), and from the 7 TeV pp run that started in March 2010 and is ongoing ($> 4 \times 10^8$ events at the moment). This study makes use of the ALICE central barrel [21], covering a range in pseudo-rapidity $|\eta| < 0.9$ and the full azimuth, the whole being placed in the large L3 solenoidal magnet which provides a nominal magnetic field of $0.5\ T$.

The strangeness signals are obtained using essentially data collected by the two main tracking detectors: the Inner Tracking System (ITS), composed of 6 cylindrical layers of high-resolution silicon detectors [22], and the cylindrical Time Projection Chamber (TPC) [23].

2.2 Topological reconstruction

The strange hadron identification is performed using a combination of displaced-vertex reconstruction, invariant mass analyses as well as single track PID methods, such as energy loss in the TPC or Time-Of-Flight (TOF) in the eponymous detector. The reconstruction of the strange and multi-strange particles hinges on their respective decays. For each particle of interest, the main characteristics and utilized decay channels are listed in Tab. 1. The anti-baryons are reconstructed similarly via the channel relying on the corresponding charge conjugates.

Particles		mass (MeV/c^2)	$c\tau$	charged decay	B.R.
Mesons	$\mathrm{K}^0_{\mathrm{S}}$	497.61	2.68 cm	$\mathrm{K}^0_{\mathrm{S}} \rightarrow \pi^+ + \pi^-$	69.2%
	ϕ	1019.46	45 fm	$\phi \rightarrow \mathrm{K}^+ + \mathrm{K}^-$	49.2%
Baryons	Λ^0 (uds)	1115.68	7.89 cm	$\Lambda^0 \rightarrow p + \pi^-$	63.9%
	Ξ^- (dss)	1321.71	4.91 cm	$\Xi^- \rightarrow \Lambda^0 + \pi^-$	99.9%
	Ω^- (sss)	1672.45	2.46 cm	$\Omega^- \rightarrow \Lambda^0 + \mathrm{K}^-$	67.8%

Table 1: Main characteristics of the reconstructed particles [24].

The guidelines of the reconstruction algorithms dedicated to ϕ, V0 and cascade structures (see below) are sketched in Fig. 1, parts *a*, *b* and *c* respectively.

The identification of ϕ consists in the association of two *primary* tracks of opposite charges, identified as kaons by TPC and possibly TOF. The $\mathrm{K}^0_{\mathrm{S}}$, Λ^0 and $\overline{\Lambda}^0$ reconstruction is grounded in the secondary vertex finding, a *V0* structure built out of two *secondary* tracks of opposite charges, compatible with coming from the same vertex within one fiducial volume. In case of

Λ^0 and $\overline{\Lambda}^0$, TPC PID is required to partially remove some combinatorial background, namely for the proton (one of the two Λ decay products, known as "daughter" particles).

The Ξ^-, $\overline{\Xi}^+$, Ω^- and $\overline{\Omega}^+$ identification is based on two secondary vertices, a Λ^0 first, which is then matched with a *secondary* track, to form a typical *cascade* structure. Here again, the matching is limited to a certain fiducial volume. The TPC PID is required for each daughter track.

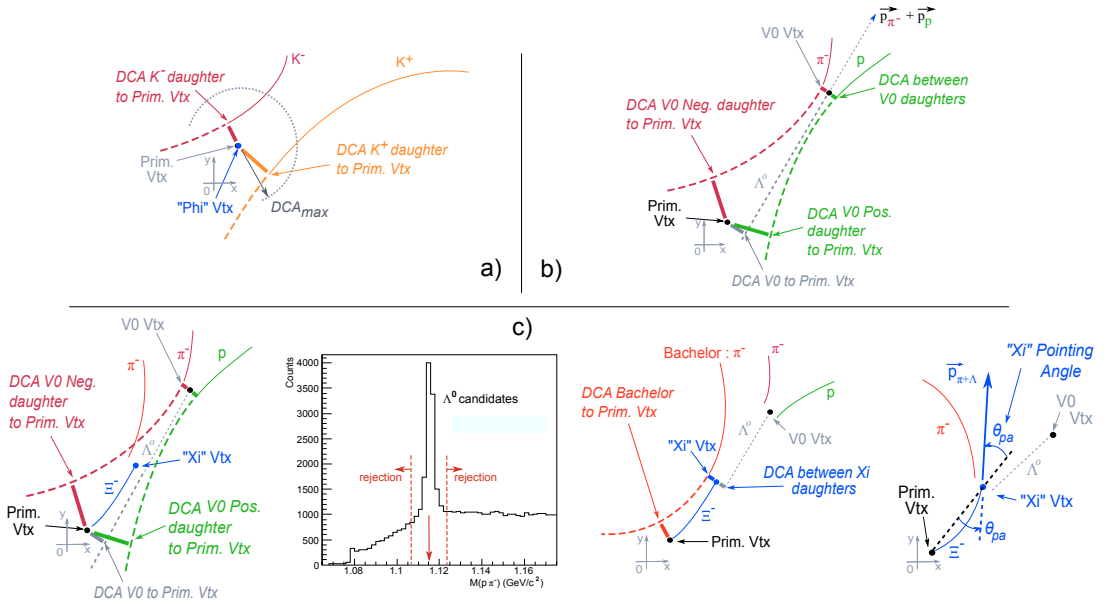

Figure 1: Reconstruction principle for (*a*) ϕ, (*b*) V0s (K^0_S, Λ^0 and $\overline{\Lambda}^0$) and (*c*) cascades (Ξ^-, $\overline{\Xi}^+$, Ω^- and $\overline{\Omega}^+$). The acronym *DCA* stands for Distance of Closest Approach.

2.3 Signal extraction

For each considered particle, we intend to extract a signal in successive p_{T} intervals. The signal extraction process using "bin-counting" method is illustrated in Fig. 2.

The signal is first approximated by a Gaussian sitting on top of a polynomial background, resulting in rough[1]estimates of the signal mean and width.

We then sample the background on each side of the signal and require both sampled regions to be more than 5σ away from the Gaussian mean. The width of the background regions varies depending on the considered particle and the transverse momentum interval chosen for the invariant mass distribution.

The sum of signal and background (S+B) is sampled in the region defined by the Gaussian mean $\pm 4\sigma$. Consequently, we make use of the areas previously sampled on the side-signal bands to assess the background B under the signal S. The signal yield $S = (S+B) - B$ is thus computed without any assumption as to its shape.

[1]The mean and width may be biased by the non-Gaussian tails of the signal. However, these quantities have the sufficient accuracy for the current purpose.

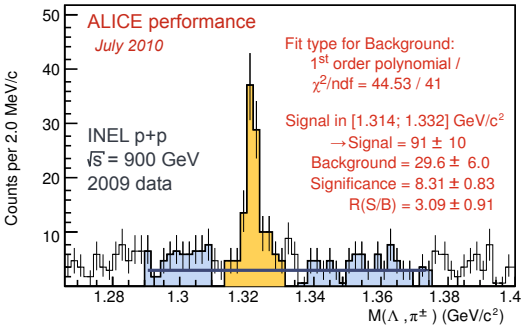

Figure 2: Signal extraction based on "bin counting" method, illustrated with the $\Xi^- + \overline{\Xi}^+$ invariant mass distribution in $1.4 < p_{\rm T}$ (GeV/c) < 2.0.

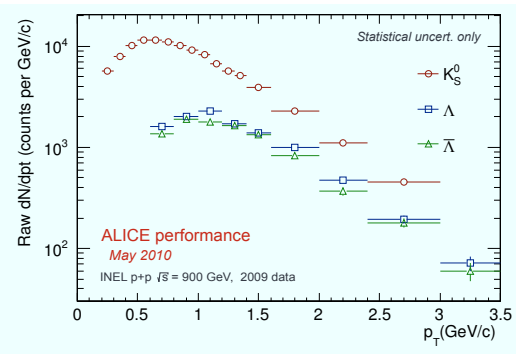

Figure 3: Raw transverse momentum spectra for $\rm K^0_S$, Λ^0 and $\overline{\Lambda}^0$ candidates (2009 data at $\sqrt{s} = 900$ GeV).

3 900 GeV and 7 TeV measurements

The results for the 2009 pp sample at 900 GeV are shown in Fig. 3 and Fig. 4. The plots show the signal counts (raw yields) for $\rm K^0_S$, Λ^0 and $\overline{\Lambda}^0$ (Fig. 3) then ϕ and $\Xi^- + \overline{\Xi}^+$ (Fig. 4), as a function of $p_{\rm T}$. The uncertainties correspond to both the statistical uncertainty related to the number of counts and the uncertainty issued from the bin-counting and fit methods needed for signal extraction.

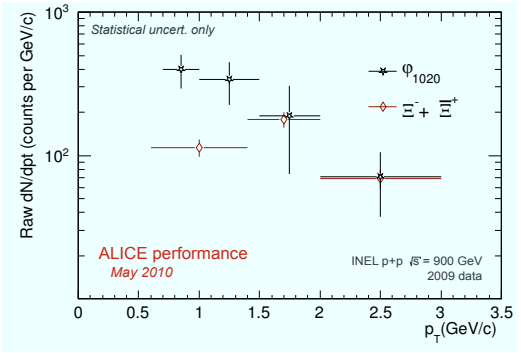

Figure 4: Raw transverse momentum spectra for ϕ and $\Xi^- + \overline{\Xi}^+$, in 2009 pp data at 900 GeV.

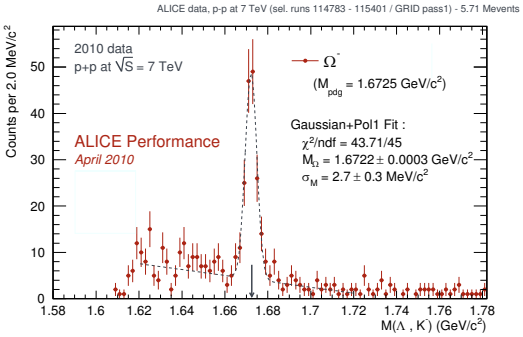

Figure 5: Invariant mass showing the Ω^- signal in 2010 pp data at 7 TeV.

A signal for the same particles can also be extracted in the pp data at 7 TeV. However, due to the available statistics, all particles and anti-particles can be studied separately and with larger counts: $\Xi^-$and $\overline{\Xi}^+$or even $\Omega^-$and $\overline{\Omega}^+$can now be discriminated, as suggested in Fig. 5.

4 Conclusion

The uncorrected spectra for strange and multi-strange hadrons are presented for the first LHC pp run at 900 GeV. Despite the limited statistics, p_{T} spectra for ϕ, $\mathrm{K}^0_{\mathrm{S}}$, Λ^0, $\overline{\Lambda}^0$ and $\Xi^- + \overline{\Xi}^+$ were obtained; the evaluation of efficiency corrections and systematic uncertainties is under finalisation.

Due to the large statistics available, the 7-TeV pp data sample enables the reconstruction of more hadron species carrying strangeness, Ω hyperons in particular as well as additional strange resonances like $\mathrm{K}^*(892)^0$ or $\Sigma^*(1385)$. This bodes well for more accurate and differential analyses such as spectra as a function of p_{T}, rapidity or event multiplicity.

References

[1] B. Alessandro (ed.) *et al.* [ALICE Collaboration], J. Phys. G **32** (2006) 1295.

[2] T. Sjöstrand, S. Mrenna and P. Z. Skands, J. High Energy Phys. 0605 (2006) 026.

[3] R. Engel, J. Ranft and S. Roesler, Phys. Rev. D**52**, (1995) 1459.

[4] F. Becattini and U. W. Heinz, Z. Phys. C**76**, (1997) 269.

[5] P. Braun-Munzinger, K. Redlich and J. Stachel, arXiv:nucl-th/0304013.

[6] T. Sjöstrand and P. Z. Skands, Eur. Phys. J. C**39**, (2005) 129.

[7] K. Werner, Nucl. Phys. Proc. Suppl. **175-176**, 81 (2008).

[8] K. Werner, I. Karpenko, T. Pierog, M. Bleicher and K. Mikhailov, arXiv:1004.0805 [nucl-th].

[9] STAR Collaboration, B. I. Abelev *et al.*, Phys. Rev. C**75**, (2007) 064901.

[10] UA5 Collaboration, R. E. Ansorge *et al.*, Nucl. Phys. B**328**, (1989) 36.

[11] UA1 Collaboration, G. Bocquet *et al.*, Phys. Lett. B**366**, (1996) 441.

[12] CDF Collaboration, F. Abe *et al.*, Phys. Rev. D**40**, (1989) 3791 RC.

[13] CDF Collaboration, D. Acosta *et al.*, Phys. Rev. D**72** (2005) 052001.

[14] UA5 Collaboration, R. E. Ansorge *et al.*, Z. Phys. C**41** (1988) 179.

[15] STAR Collaboration, J. Adams *et al.*, Phys. Lett. B**612** (2005) 181.

[16] STAR Collaboration, B. I. Abelev *et al.*, Phys. Rev. C**79** (2009) 064903.

[17] E735 Collaboration, T. Alexopoulos *et al.*, Z. Phys. C**67** (1995) 411.

[18] CDF Collaboration, public note, CDF/PUB/QCD/PUBLIC/10084 (2010), www-cdf.fnal.gov.

[19] B. Hippolyte, Eur. Phys. J. C **62** (2009) 237 [arXiv:0901.3176 [hep-ex]].

[20] L. Evans and P. Bryant, (ed.), JINST 3 **64**, (2008) S08001.

[21] K. Aamodt *et al.* [ALICE Collaboration], JINST **3** (2008) S08002.

[22] K. Aamodt *et al.* [ALICE Collaboration], JINST **5** (2010) P03003 [arXiv:1001.0502 [physics.ins-det].

[23] J. Alme *et al.* [ALICE Collaboration], arXiv:1001.1950 [physics.ins-det].

[24] C. Amsler *et al.* (Particle Data Group), Phys. Lett. B **667**, (2008) 1.